UNIVERSITY OF HELSINKI

https://helda.helsinki.fi

Substantial large-scale feedbacks between natural aerosols and climate

Scott, Catherine; Arnold, Stephen; Monks, Sarah; Asmi, Ari; Paasonen, Pauli ...

2017-12-04
Nature Publishing Group
http://hdl.handle.net/10138/308161
Scott, C, Arnold, S, Monks, S, Asmi, A, Paasonen, P & Spracklen, D 2017, 'Substantial large-scale feedbacks between natural aerosols and climate', Nature Geoscience, vol. 11, no. 1, pp. 44-48. https://doi.org/10.1038/s41561-017-0020-5

Downloaded from Helda, University of Helsinki institutional repository. https://helda.helsinki.fi
This is an electronic reprint of the original article.
This reprint may differ from the original in pagination and typographic detail.
Please cite the original version.

Substantial large scale feedbacks between natural aerosols and climate

Scott, C. E.[1*], Arnold, S.R. [1], Monks, S.A.[2,3], Asmi, A.[4], Paasonen, P.[4,5], Spracklen, D.V. [1*]

[1]Institute for Climate and Atmospheric Science, School of Earth and Environment, University of Leeds, Leeds, UK

[2]Cooperative Institute for Research in Environmental Sciences, University of Colorado, Boulder, Colorado, USA

[3]Chemical Sciences Division, NOAA Earth System Research Laboratory, Boulder, Colorado, USA

[4] Department of Physics, University of Helsinki, FI-00014, Finland,

[5]International Institute for Applied Systems Analysis, A-2361 Laxenburg, Austria

*email: C.E.Scott@leeds.ac.uk; D.V.Spracklen@leeds.ac.uk

The terrestrial biosphere is an important source of natural aerosol. Natural aerosol sources alter climate, but are also strongly controlled by climate, leading to the potential for natural aerosol-climate feedbacks. Here we use a global aerosol model to make the first assessment of terrestrial natural aerosol-climate feedbacks, constrained by observations of aerosol number. We find that warmer than average temperatures are associated with higher than average number concentrations of large (> 100 nm diameter) particles, particularly during the summer. This relationship is well reproduced by the model and is driven by both meteorological variability and variability in natural aerosol from biogenic and landscape fire sources. We find that the calculated extra-tropical annual mean aerosol radiative effect (both direct and indirect) is

negatively related to the observed global temperature anomaly, and is driven by a positive relationship between temperature and emission of natural aerosol. The extra-tropical aerosol-climate feedback is estimated to be -0.14 Wm^{-2} K^{-1} for landscape fire aerosol, greater than the -0.03 Wm^{-2} K^{-1} estimated for biogenic secondary organic aerosol. These feedbacks are comparable in magnitude to other biogeochemical feedbacks, highlighting the need for natural aerosol feedbacks to be included in climate simulations.

The terrestrial biosphere regulates atmospheric composition and climate by altering the exchange of energy, water and trace gases between the surface and atmosphere[1]. The terrestrial biosphere is an important source of natural aerosols[2] from vegetation fires and biogenic volatile organic compounds (BVOCs) which can form secondary organic aerosol (SOA)[3]. These natural sources can dominate ambient aerosol in tropical[4-7], temperate[8,9] and boreal[10] environments. Atmospheric aerosol alters the Earth's climate by absorbing and scattering radiation (direct radiative effect) and through altering the albedo of clouds (first aerosol indirect effect)[11]. Because natural aerosol constitutes a major fraction of ambient aerosol it can have important radiative effects[12-15]. The physical and biological process that control natural aerosol sources are highly sensitive to climate[2]. For example, changes to climate drive large changes in fire[16-18], BVOC[19] and dust[20] emissions. These interactions between natural aerosol and climate create the potential for natural aerosol-climate feedbacks.

A number of natural aerosol-climate feedbacks have been proposed. The first proposed, and maybe best known, involves ocean biology and emission of di-methylsulfide[21]. Terrestrial aerosol-climate feedbacks have also been suggested[1].

Warmer temperatures drive increased BVOC emissions and increased SOA concentrations, which lead to a negative radiative effect and a cooling impact on climate[22]. Warmer temperatures also lead to increased fires and associated aerosol emissions[16] with impacts on climate. Observations of increased aerosol concentrations with increasing ambient temperatures have been attributed to these interactions[23,24]. However, the magnitude of natural aerosol feedbacks has rarely been assessed, although large projected changes in natural aerosol under a warming climate suggest that they could be substantial[2]. Here we explore the potential magnitude of aerosol feedbacks for two terrestrial natural aerosol sources with important climate impacts[12]: biogenic SOA and landscape fire aerosol.

Exploring natural aerosol – temperature interactions

To explore the potential for natural aerosol-climate feedbacks, we analysed long-term measurements of aerosol number made at 11 continental locations (Supplementary Fig. 1) mostly across northern hemisphere mid-latitudes[24]. We used the number concentration of particles with dry diameter larger than 100 nm (N_{100}) as a proxy for concentrations of cloud condensation nuclei (CCN)[25]. Particles with dry diameters larger than 100 nm are also those that are able to scatter radiation efficiently in the atmosphere.

At most of these locations, N_{100} is positively related to local surface temperature (Supplementary Fig. 2) as reported previously[24]. We find that a global aerosol microphysics model[26] (see Methods) reproduces this observed relationship well (Supplementary Fig. 2). To further explore the relationship between surface temperature and N_{100}, we de-seasonalised both variables. Figure 1 shows the N_{100} anomaly as a function of anomaly in local surface temperature. In summer we find that most locations exhibit a strong positive relationship between temperature

anomaly and anomaly in N_{100}, with little or no relationship in winter. This means that in summer, days that are warmer than average typically have higher than average N_{100}. The global model, analysed in the same way as the observations, reproduces the observed relationships (Fig. 1). The summertime mean observed sensitivity between N_{100} and temperature, calculated across all observation stations, is +51.3±5.9 cm^{-3} K^{-1} (linear regression based on 500 bootstrap samples) and is well reproduced by the model (+43.5±4.2 cm^{-3} K^{-1}). The relative anomaly in particle number shows a similar relationship that is also well reproduced by the model (Supplementary Fig. 3). This suggests that the model captures the processes responsible for driving the observed temperature-aerosol relationships.

The observed relationship between temperature and aerosol number could be due to interactions between natural aerosol sources and climate. However, it could also be due to processes unrelated to natural aerosol sources. For example, warmer temperatures could be associated with lower rainfall, and therefore reduced aerosol loss via wet deposition. Or warmer temperatures could be related to transport of southerly air masses towards the measurement locations, bringing more polluted air with high aerosol concentrations.

To help interpret the observed relationships, we analysed multiple simulations from the atmospheric aerosol model in which we individually switch off interannual variability in natural aerosol emissions or meteorology (see Methods). At all locations, we find that the simulated relationship between N_{100} anomaly and temperature anomaly breaks down (sensitivity of N_{100} to temperature reduced to +5.0±1.6 cm^{-3} K^{-1}) when we remove interannual variability in simulated meteorology (i.e., the simulation uses repeating 1997 meteorological data). This suggests that meteorology is an important mechanism driving the observed relationship between

anomalies in N_{100} and temperature. Simulations where we remove interannual variability in natural aerosol emissions have less impact on the simulated relationship between N_{100} and temperature, with sensitivity reducing to +41.9±4.2 cm^{-3} K^{-1} for fixed fire and +40.9±4.0 cm^{-3} K^{-1} for fixed BVOC emissions (Supplementary Fig. 4). We also find that if we increase simulated SOA formation from BVOCs (by a factor 5) the relationship between N_{100} and temperature further breaks down at warm temperature anomalies (Supplementary Fig. 4). This demonstrates that the relationship between N_{100} and temperature is sensitive to the treatment of SOA in the model and suggests that this treatment is adequately represented in the control simulation. Overall our analysis suggests that whilst meteorology is the dominant driver of observed relationships between temperature and aerosol number, variability in natural aerosol emission also contributes. Our realistic simulation of the observed relationships between aerosol and temperature suggests that our model treatment of fire emissions and SOA[14] are adequate to simulate the main interactions that are important for this study.

Interannual variability in aerosol radiative effects

Using the multi-annual simulations of global aerosol, we explore how natural aerosol sources alter the internannual variability in top-of-atmosphere aerosol radiative effect. We focus on the aerosol direct radiative effect (DRE) and first aerosol indirect effect (AIE), also known as the cloud albedo effect[11]. Other interactions between aerosol and cloud are likely, but are highly uncertain[27]. Over the period 1997 to 2007, the global annual mean DRE has a standard deviation of 0.025 W m^{-2} whereas the AIE has a standard deviation of 0.017 W m^{-2} (Supplementary Figure 5). In this control simulation, year to year variability in fire emissions are prescribed from the Global Fire Emissions Dataset version 3 (GFED3)[28] and BVOC emissions are

125 calculated using MEGAN version 2.1 (ref.[29]). To isolate the contribution of different
126 aerosol sources to this variability in the aerosol RE we individually switch off natural
127 aerosol - climate couplings (see Methods). We then use the difference between the
128 control simulation and the simulation where the interannual variability of the natural
129 aerosol source has been switched off to calculate the variability caused by each
130 natural aerosol source. Figure 2 shows the interannual variability in simulated
131 aerosol RE due to variability in biogenic SOA and fire emissions. Variability in fire
132 aerosol causes interannual variability in both DRE and AIE of greater than 0.5 W m^{-2}
133 over and downwind of regions of tropical and boreal fires. Interannual variability in
134 biogenic SOA causes smaller variability in RE, with variability of up to 0.2 W m^{-2} over
135 the SE United States and tropical forest regions. Landscape fires have also been
136 shown to control interannual variability in regional surface carbonaceous aerosol
137 concentrations[9] and aerosol optical depth[30].

138 Figure 2 shows that some of the largest simulated radiative impacts caused by
139 variability in natural aerosol are in the tropics. However, our understanding of
140 atmospheric composition and emissions of natural aerosol in the tropics is still poor.
141 There are very few long-term studies of aerosol size distribution in the tropical
142 atmosphere and none of our 11 stations are in the tropics (defined here as 20°S to
143 20°N). The tropics are thought to be the dominant source of both BVOC[29] and fire[28]
144 emissions. However, there have been few studies of BVOC emissions in the tropics.
145 A study in the Amazon, confirmed the importance of temperature, light and leaf
146 phenology in driving BVOC emissions but also suggested our mechanistic
147 understanding of BVOC emissions in the tropics is still limited[31]. The chemical
148 composition of monoterpene emissions in the tropics may also vary with
149 temperature, with reactive isomers being enriched at high temperatures[32,33] with

potential consequences for SOA. For these reasons we focus on the extra-tropical (>20°S and >20°N) RE, where there is less uncertainty in BVOC emissions and we have observations to constrain the sensitivity of the aerosol model to natural aerosol.

We explored the control on the variability in aerosol RE over the period 1997 to 2007 (see Methods). We find that there is a negative correlation between global (land and ocean) surface temperature anomaly and the anomaly in extra-tropical annual mean DRE (Pearson's r = -0.74, $P<0.01$) and AIE (r=-0.52, $P<0.1$) (Supplementary Table 1). Figure 3 shows the anomaly in RE due to variability in biogenic SOA and fire aerosol as a function of the anomaly in annual global temperature (see Methods). We find an even stronger negative correlation between the global temperature anomaly and anomaly in extra-tropical annual mean RE from biogenic SOA, both for the DRE (r=-0.76, $P<0.01$) and AIE (r=-0.71, $P<0.01$). Simulated emissions of BVOC are strongly controlled by temperature[29]; we find a strong positive correlation between annual extra-tropical BVOC emission and global temperature anomaly (monoterpene r=0.78; isoprene r=0.79) (Supplementary Figure 7). Warmer than average years drive increased BVOC emissions leading to increased formation of SOA, which results in a stronger negative DRE and AIE.

We also simulate a negative correlation between global temperature anomaly and the anomaly in the extra-tropical RE from fire, both for the DRE (r=-0.5, $P<0.1$) and AIE (r=-0.51, $P<0.05$). We find a positive correlation between annual extra-tropical particulate emission from landscape fires and global temperature anomaly (r=0.39) (Supplementary Fig. 7). The correlation between temperature anomaly and RE from fires is weaker compared to BVOC, due to this weaker correlation between temperature and fire emission. Global fire activity is governed by a complex suite of climate, natural and human ignition sources and available fuel[18]. Whilst years with

175 warm temperature anomalies are associated with greater fire emissions, other
176 climate variables such as rainfall and relative humidity are also important[18,34].

177 **Diagnosing natural aerosol-climate feedbacks**

178 We used the relationship between RE and global temperature anomaly to estimate
179 the aerosol radiative feedback (λ) for the different natural aerosol sources, following
180 the framework of previous work[1] (see Methods). In this framework climate feedbacks
181 are expressed in common units of W m^{-2} K^{-1} and are shown in Figure 4. We estimate
182 that fire results in an extra-tropical direct aerosol radiative feedback of -0.09±0.06 W
183 m^{-2} K^{-1} and an extra-tropical indirect aerosol radiative feedback of -0.06±0.03 W m^{-2}
184 K^{-1}. We estimate a smaller radiative feedback due to biogenic SOA, with an extra-
185 tropical direct radiative feedback of -0.02±0.01 W m^{-2} K^{-1} and an extra-tropical
186 indirect aerosol radiative feedback of -0.007±0.002 W m^{-2} K^{-1}.

187 Figure 4 also shows our estimates of the global radiative feedbacks. The global
188 aerosol feedback for fire aerosol is relatively similar to that calculated for the extra-
189 tropics. In contrast, the global biogenic SOA feedback is about double the strength of
190 that calculated in the extra-tropics (Fig. 4). We note that we have no observational
191 constraint of the natural aerosol feedback in the tropics, and so these global
192 estimates are unconstrained. Long-term observations of BVOC emissions and
193 aerosol concentrations in the tropics are urgently needed.

194 The stronger fire aerosol radiative feedback compared to the biogenic SOA feedback
195 is primarily due to the stronger interannual variability of fire emissions compared to
196 BVOCs. The coefficient of variation (standard deviation divided by mean) for global
197 particulate emission from fire is 19.6% (Supplementary Fig. 7 and Methods). The
198 simulated coefficient of variation for BVOC emissions is substantially smaller both for
199 isoprene emissions (2.9%) and for monoterpene emissions (2.4%). Our simulated

interannual variability in BVOC emissions and biogenic SOA matches previous work[35]. The absolute variability in both BVOC and particulate emissions from fire is greatest in the tropics, but the extra-tropics exhibits greater fractional variability (Supplementary Fig. 6 and 7).

We find that the direct radiative feedback is stronger than the indirect radiative feedback for both natural aerosol sources. This behaviour is particularly true for biogenic SOA where the direct aerosol feedback is more than a factor 3 greater than the indirect aerosol feedback. We note that our estimated direct aerosol feedback for fires will depend on the net DRE of fire aerosol which is uncertain[36]. The relatively weak aerosol indirect feedback for biogenic SOA is due to the AIE being relatively insensitive to emission of BVOC[12,14]. The global biogenic SOA feedback from aerosol indirect effect that we estimate here (-0.013 ± 0.002 W m^{-2} K^{-1}) is similar to the global mean value of -0.01 W m^{-2} K^{-1} inferred from selected observations[24].

Our estimate of natural aerosol - climate feedbacks is applicable for the present day and may be different in future or past climates. Climate change and increased atmospheric carbon dioxide concentrations will alter the amount and type of vegetation[37,38], altering both BVOC[29] and fire emissions[39,40]. Changes in environmental factors in a warming climate may lead to stressed vegetation and additional BVOC emissions, potentially creating stronger couplings between vegetation, aerosol and climate[41]. Increased CO_2 concentrations may alter BVOC emissions[29], altering biogenic SOA and associated feedbacks. Feedbacks can also be directly altered by human activity. Land-use change and land management have altered BVOC and fire emissions since pre-human times[42]. Anthropogenic aerosol suppresses natural aerosol - climate interactions[43], meaning natural aerosol - climate feedbacks may strengthen with future reductions in anthropogenic aerosol

emissions. Additional feedbacks between the biosphere, BVOC, fire emissions and climate operating through precipitation and soil moisture are possible, but are not included here.

The strength of natural aerosol feedbacks is comparable in magnitude to a range of other biogeochemical feedbacks[1] and is opposite in sign to the global snow-albedo feedback which has been estimated as +0.1 $W m^{-2} K^{-1}$ (ref.[44]). Our findings suggest that natural aerosol-climate feedbacks may play a role in moderating net temperature response to CO_2-driven or other external forcings, and should be included in fully-coupled simulations of past and future climate.

247 **References**

248

249 1 Arneth, A. *et al.* Terrestrial biogeochemical feedbacks in the climate system.
250 *Nat. Geosci.* **3**, 525-532, doi:10.1038/ngeo905 (2010).

251 2 Carslaw, K. S. *et al.* A review of natural aerosol interactions and feedbacks
252 within the Earth system. *Atmos. Chem. Phys.* **10**, 1701-1737,
253 doi:10.5194/acp-10-1701-2010 (2010).

254 3 Hallquist, M. *et al.* The formation, properties and impact of secondary organic
255 aerosol: current and emerging issues. *Atmos. Chem. Phys.* **9**, 5155-5236
256 (2009).

257 4 Poschl, U. *et al.* Rainforest Aerosols as Biogenic Nuclei of Clouds and
258 Precipitation in the Amazon. *Science* **329**, 1513-1516,
259 doi:10.1126/science.1191056 (2010).

260 5 Martin, S. T. *et al.* SOURCES AND PROPERTIES OF AMAZONIAN
261 AEROSOL PARTICLES. *Reviews of Geophysics* **48**,
262 doi:10.1029/2008rg000280 (2010).

263 6 Martin, S. T. *et al.* Introduction: Observations and Modeling of the Green
264 Ocean Amazon (GoAmazon2014/5). *Atmos. Chem. Phys.* **16**, 4785-4797,
265 doi:10.5194/acp-16-4785-2016 (2016).

266 7 Andreae, M. O. *et al.* The Amazon Tall Tower Observatory (ATTO): overview
267 of pilot measurements on ecosystem ecology, meteorology, trace gases, and
268 aerosols. *Atmos. Chem. Phys.* **15**, 10723-10776, doi:10.5194/acp-15-10723-
269 2015 (2015).

270 8 Goldstein, A. H., Koven, C. D., Heald, C. L. & Fung, I. Y. Biogenic carbon and
271 anthropogenic pollutants combine to form a cooling haze over the
272 southeastern United States. *Proceedings of the National Academy of*
273 *Sciences of the United States of America* **106**, 8835-8840,
274 doi:10.1073/pnas.0904128106 (2009).

275 9 Spracklen, D. V. *et al.* Wildfires drive interannual variability of organic carbon
276 aerosol in the western US in summer. *Geophys. Res. Lett.* **34**,
277 doi:10.1029/2007gl030037 (2007).

278 10 Tunved, P. *et al.* High natural aerosol loading over boreal forests. *Science*
279 **312**, 261-263, doi:10.1126/science.1123052 (2006).

280 11 Twomey, S. Aerosols, clouds and radiation. *Atmospheric Environment* **25**,
281 2435-2442 (1991).

282 12 Rap, A. *et al.* Natural aerosol direct and indirect radiative effects. *Geophys.*
283 *Res. Lett.* **40**, 3297-3301, doi:10.1002/grl.50441 (2013).

284 13 Satheesh, S. K. & Moorthy, K. K. Radiative effects of natural aerosols: A
285 review. *Atmospheric Environment* **39**, 2089-2110,
286 doi:10.1016/j.atmosenv.2004.12.029 (2005).

14 Scott, C. E. *et al.* The direct and indirect radiative effects of biogenic secondary organic aerosol. *Atmos. Chem. Phys.* **14**, 447-470, doi:10.5194/acp-14-447-2014 (2014).

15 Unger, N. Human land-use-driven reduction of forest volatiles cools global climate. *Nat. Clim. Chang.* **4**, 907-910, doi:10.1038/nclimate2347 (2014).

16 Spracklen, D. V. *et al.* Impacts of climate change from 2000 to 2050 on wildfire activity and carbonaceous aerosol concentrations in the western United States. *J. Geophys. Res.-Atmos.* **114**, doi:10.1029/2008jd010966 (2009).

17 Ward, D. S. *et al.* The changing radiative forcing of fires: global model estimates for past, present and future. *Atmos. Chem. Phys.* **12**, 10857-10886, doi:10.5194/acp-12-10857-2012 (2012).

18 Jolly, W. M. *et al.* Climate-induced variations in global wildfire danger from 1979 to 2013. *Nat. Commun.* **6**, 11, doi:10.1038/ncomms8537 (2015).

19 Heald, C. L. *et al.* Predicted change in global secondary organic aerosol concentrations in response to future climate, emissions, and land use change. *J. Geophys. Res.-Atmos.* **113**, 16, doi:10.1029/2007jd009092 (2008).

20 Mahowald, N. M. *et al.* Change in atmospheric mineral aerosols in response to climate: Last glacial period, preindustrial, modern, and doubled carbon dioxide climates. *J. Geophys. Res.-Atmos.* **111**, 22, doi:10.1029/2005jd006653 (2006).

21 Charlson, R. J., Lovelock, J. E., Andreae, M. O. & Warren, S. G. OCEANIC PHYTOPLANKTON, ATMOSPHERIC SULFUR, CLOUD ALBEDO AND CLIMATE. *Nature* **326**, 655-661, doi:10.1038/326655a0 (1987).

22 Kulmala, M. *et al.* A new feedback mechanism linking forests, aerosols, and climate. *Atmos. Chem. Phys.* **4**, 557-562 (2004).

23 Lihavainen, H., Asmi, E., Aaltonen, V., Makkonen, U. & Kerminen, V. M. Direct radiative feedback due to biogenic secondary organic aerosol estimated from boreal forest site observations. *Environ. Res. Lett.* **10**, 8, doi:10.1088/1748-9326/10/10/104005 (2015).

24 Paasonen, P. *et al.* Warming-induced increase in aerosol number concentration likely to moderate climate change. *Nat. Geosci.* **6**, 438-442, doi:10.1038/ngeo1800 (2013).

25 Dusek, U. *et al.* Size Matters More Than Chemistry for Cloud-Nucleating Ability of Aerosol Particles. *Science* **312**, 1375-1378, doi:10.1126/science.1125261 (2006).

26 Mann, G. W. *et al.* Description and evaluation of GLOMAP-mode: a modal global aerosol microphysics model for the UKCA composition-climate model. *Geoscientific Model Development* **3**, 519-551, doi:10.5194/gmd-3-519-2010 (2010).

27 Lohmann, U. & Feichter, J. Global indirect aerosol effects: a review. *Atmos. Chem. Phys.* **5**, 715-737 (2005).

28 van der Werf, G. R. *et al.* Global fire emissions and the contribution of deforestation, savanna, forest, agricultural, and peat fires (1997-2009).

Atmos. Chem. Phys. **10**, 11707-11735, doi:10.5194/acp-10-11707-2010 (2010).

29 Guenther, A. B. *et al.* The Model of Emissions of Gases and Aerosols from Nature version 2.1 (MEGAN2.1): an extended and updated framework for modeling biogenic emissions. *Geoscientific Model Development* **5**, 1471-1492, doi:10.5194/gmd-5-1471-2012 (2012).

30 Voulgarakis, A. *et al.* Interannual variability of tropospheric trace gases and aerosols: The role of biomass burning emissions. *J. Geophys. Res.-Atmos.* **120**, 7157-7173, doi:10.1002/2014jd022926 (2015).

31 Alves, E. G. *et al.* Seasonality of isoprenoid emissions from a primary rainforest in central Amazonia. *Atmos. Chem. Phys.* **16**, 3903-3925 (2016).

32 Jardine, K. J. *et al.* Monoterpene 'thermometer' of tropical forest-atmosphere response to climate warming. *Plant, Cell & Environment* **40**, 441-452, doi:10.1111/pce.12879 (2017).

33 Jardine, A. B. *et al.* Highly reactive light-dependent monoterpenes in the Amazon. *Geophys. Res. Lett.* **42**, 1576-1583, doi:10.1002/2014GL062573 (2015).

34 van der Werf, G. R., Randerson, J. T., Giglio, L., Gobron, N. & Dolman, A. J. Climate controls on the variability of fires in the tropics and subtropics. *Glob. Biogeochem. Cycle* **22**, 13, doi:10.1029/2007gb003122 (2008).

35 Tsigaridis, K., Lathiere, J., Kanakidou, M. & Hauglustaine, D. A. Naturally driven variability in the global secondary organic aerosol over a decade. *Atmos. Chem. Phys.* **5**, 1891-1904 (2005).

36 Myhre, G. *et al.* Radiative forcing of the direct aerosol effect from AeroCom Phase II simulations. *Atmos. Chem. Phys.* **13**, 1853-1877, doi:10.5194/acp-13-1853-2013 (2013).

37 Zhu, Z. C. *et al.* Greening of the Earth and its drivers. *Nat. Clim. Chang.* **6**, 791-795, doi:10.1038/nclimate3004 (2016).

38 Zaehle, S., Jones, C. D., Houlton, B., Lamarque, J. F. & Robertson, E. Nitrogen Availability Reduces CMIP5 Projections of Twenty-First-Century Land Carbon Uptake. *Journal of Climate* **28**, 2494-2511, doi:10.1175/jcli-d-13-00776.1 (2015).

39 Kloster, S. & Lasslop, G. Historical and future fire occurrence (1850 to 2100) simulated in CMIP5 Earth System Models. *Glob. Planet. Change* **150**, 58-69, doi:10.1016/j.gloplacha.2016.12.017 (2017).

40 Hantson, S. *et al.* The status and challenge of global fire modelling. *Biogeosciences* **13**, 3359-3375, doi:10.5194/bg-13-3359-2016 (2016).

41 Zhao, D. F. *et al.* Environmental conditions regulate the impact of plants on cloud formation. *Nat. Commun.* **8**, 8, doi:10.1038/ncomms14067 (2017).

42 Heald, C. L. & Spracklen, D. V. Land Use Change Impacts on Air Quality and Climate. *Chem. Rev.* **115**, 4476-4496, doi:10.1021/cr500446g (2015).

43 Spracklen, D. V. & Rap, A. Natural aerosol-climate feedbacks suppressed by anthropogenic aerosol. *Geophys. Res. Lett.* **40**, 5316-5319, doi:10.1002/2013gl057966 (2013).

44 Thackeray, C. W. & Fletcher, C. G. Snow albedo feedback: Current knowledge, importance, outstanding issues and future directions. *Prog. Phys. Geogr.* **40**, 392-408, doi:10.1177/0309133315620999 (2016).

Acknowledgements

We acknowledge support from the Natural Environment Research Council (NE/K015966/1) and EU Horizon 2020 (SC5-01-2014; grant agreement no 641816). This work used the ARCHER UK National Supercomputing Service (http://www.archer.ac.uk).

Author contributions

All authors contributed to the research design. CS and SM performed model simulations. AA and PP provided observational data. CS, DS and SA analysed the data. All authors contributed to scientific discussions and helped to write the manuscript.

Additional information

Supplementary information is available in the online version of the paper. Correspondence and requests for materials should be sent to CS.

Competing financial interests

The authors declare no competing financial interests.

Figure captions

Figure 1. Relationship between particle number anomaly and temperature anomaly. The particle number anomaly is for particles greater than 100 nm diameter (N_{100}). Winter (top panels: a, b) and summer (bottom panels: c, d) are shown for observations (left: a, c) and model (right: b, d). Each observation is represented by a

point (left), whilst the lines represent the median N_{100} anomaly per 2 K temperature anomaly bin. Different locations are indicated by the different lines (see key). All stations except one are in the Northern Hemisphere where winter is December to February and summer is July to August. For the one station in the Southern Hemisphere we show July to August as winter and December to February as summer.

Figure 2. Interannual variability in aerosol radiative effect (RE). (a, b) Direct radiative effect, (c, d) aerosol indirect effect shown for biogenic SOA (a, c) and fire (b, d). Numbers on the panels show the standard deviation in global annual mean RE over the period 1997 - 2007.

Figure 3. Relationship between aerosol radiative effect (RE) and global temperature anomaly. (a) Direct radiative effect, (b) aerosol indirect effect shown for biogenic SOA (blue) and fire (red). Symbols show results for the extra-tropics (>20°N and >20°S). Linear fits are shown for the extra-tropics (solid line) and at the global scale (dashed line). Number on panel shows correlation (r) between RE and temperature anomaly. Temperature anomalies are calculated relative to a 1971 to 2000 climatology.

Figure 4. Simulated natural aerosol feedback. Values are shown for biogenic SOA (blue) and fire (red). Solid bars show the extra-tropical feedback (>20°N and >20°S), dashed bars show the global feedback. Error bar shows standard error in the estimated feedback (based on 500 bootstrap samples).

Methods

Observations: We used long term observations of the number concentration of particles larger than 100 nm in diameter (N_{100}) and surface temperature from 11

surface stations. The observations are as described in ref.[24]. We de-seasonalised both N_{100} and temperature through subtracting the long-term monthly mean from the original data. We calculated the sensitivity of N_{100} to surface temperature between an anomaly of -10 K and +10 K.

Aerosol model: We used the TOMCAT chemical transport model coupled to the GLOMAP-mode aerosol microphysics model[26] to simulate the distribution of atmospheric aerosol over the period 1997-2007. Fire emissions were from GFEDv3, based on burned area, active fire detections and plant productivity from the MODerate resolution Imaging Spectroradiometer (MODIS)[28]. Emissions of isoprene and monoterpenes were calculated using MEGANv2.1 (ref.[29]) in the Community Land Model (CLMv4.5). Emissions depend on the distribution of vegetation, CO_2 concentration, solar radiation, temperature and moisture. Anthropogenic aerosol emissions and precursors were from the MACCity dataset[45]. Other natural aerosol and aerosol precursor emissions include oceanic DMS emissions calculated using a sea-air transfer velocity[46] and a sea surface concentration database[47], sea-spray emissions[48] and volcanic sulphur emissions[49]. GLOMAP was forced with ERA-Interim analyses from the European Centre for Medium Range Weather Forecasts (ECMWF). We use offline oxidant concentrations from the TOMCAT chemical transport model. Here GLOMAP has a horizontal resolution of 2.8°×2.8° and 31 vertical levels between the surface and 10 hPa. The model simulates aerosol component mass and number concentration (two-moment modal) in seven lognormal modes: hygroscopic nucleation, Aitken, accumulation, coarse, and non-hygroscopic Aitken, accumulation and coarse modes. The modal version of the model matches a more computationally expensive sectional scheme[50]. Secondary organic aerosol (SOA) is formed from the oxidation of monoterpenes and isoprene

449 and is treated as described in ref.[14]. The oxidation products of monoterpenes are
450 able to participate in new particle formation[51] and growth whereas the oxidation
451 products of isoprene contribute only to condensational growth. A control simulation
452 where emissions and meteorology varied according to simulation year was
453 compared against simulations where one specific emission or process was fixed to
454 1997 values. These were a) anthropogenic emissions, b) biogenic VOC emissions,
455 c) landscape fire emissions, d) ERA-Interim fields. All simulations were run for the
456 period 1997 to 2007.

457 **Radiation model**: Top-of-atmosphere, all-sky aerosol radiative effects (RE) were
458 calculated using the Suite of Community Radiative Transfer codes (SOCRATES)[52].
459 We calculated the direct radiative effect (DRE) and the aerosol indirect effect (AIE)
460 resulting from changes to cloud droplet number concentration. Full details are
461 provided in ref.[14].

462 Aerosol RE were calculated for all five aerosol model simulations that are described
463 above. The global annual mean RE was calculated for each simulation. The anomaly
464 in global annual mean radiative effect was calculated with respect to the start year of
465 the simulation (1997). We then calculated global annual mean RE anomaly for each
466 emission or process as the difference in global mean RE anomaly between the
467 control simulation and the simulation where that process had been fixed to 1997
468 values. The sum of RE anomaly from the four simulations agreed with the RE
469 anomaly from the control simulation to within 2%.

470 **Climate feedback:** Global annual temperature anomalies (ΔT) are from the National
471 Oceanic and Atmospheric Administration (NOAA). We used the NOAA Merged Land
472 Ocean Global Surface Temperature Analysis Dataset (NOAAGlobalTemp v4.0.1)[53],
473 a spatially gridded (5°× 5°) global surface temperature dataset. Temperature

anomalies were calculated over land and ocean with respect to the 1971 to 2000 climatology. The Pearson's correlation (r) between ΔRE and ΔT was calculated for each simulation.

We calculate the climate feedback (λ) following previous work[1]. Climate feedbacks, expressed in units of W m^{-2} K^{-1}, are calculated for each natural aerosol as the change in top-of-atmosphere radiative effect (ΔRE) divided by the change in global mean surface temperature (ΔT) (i.e., λ = ΔRE / ΔT), determined from the gradient of the best fit line between the ΔRE and ΔT. Uncertainty in the calculated feedback is estimated using a bootstrapping approach, based on 500 bootstrap samples.

Data availability: The NOAA Merged Land Ocean Global Surface Temperature Analysis Dataset (NOAAGlobalTemp v4.0.1) is available online (https://www.ncdc.noaa.gov/data-access/marineocean-data/noaa-global-surface-temperature-noaaglobaltemp). Data from our model simulations are available upon request.

Code availability: A request for the code used to generate these results can be made via http://www.ukca.ac.uk/wiki/index.php/Main_Page

45 Granier, C. *et al.* Evolution of anthropogenic and biomass burning emissions of air pollutants at global and regional scales during the 1980-2010 period. *Clim. Change* **109**, 163-190, doi:10.1007/s10584-011-0154-1 (2011).

46 Nightingale, P. D. *et al.* In situ evaluation of air-sea gas exchange parameterizations using novel conservative and volatile tracers. *Glob. Biogeochem. Cycle* **14**, 373-387, doi:10.1029/1999GB900091 (2000).

47 Kettle, A. J. & Andreae, M. O. Flux of dimethylsulfide from the oceans: A comparison of updated data sets and flux models. *Journal of Geophysical Research: Atmospheres* **105**, 26793-26808, doi:10.1029/2000JD900252 (2000).

48 Gong, S. L. A parameterization of sea-salt aerosol source function for sub- and super-micron particles. *Glob. Biogeochem. Cycle* **17**, 1097, doi:10.1029/2003GB002079 (2003).

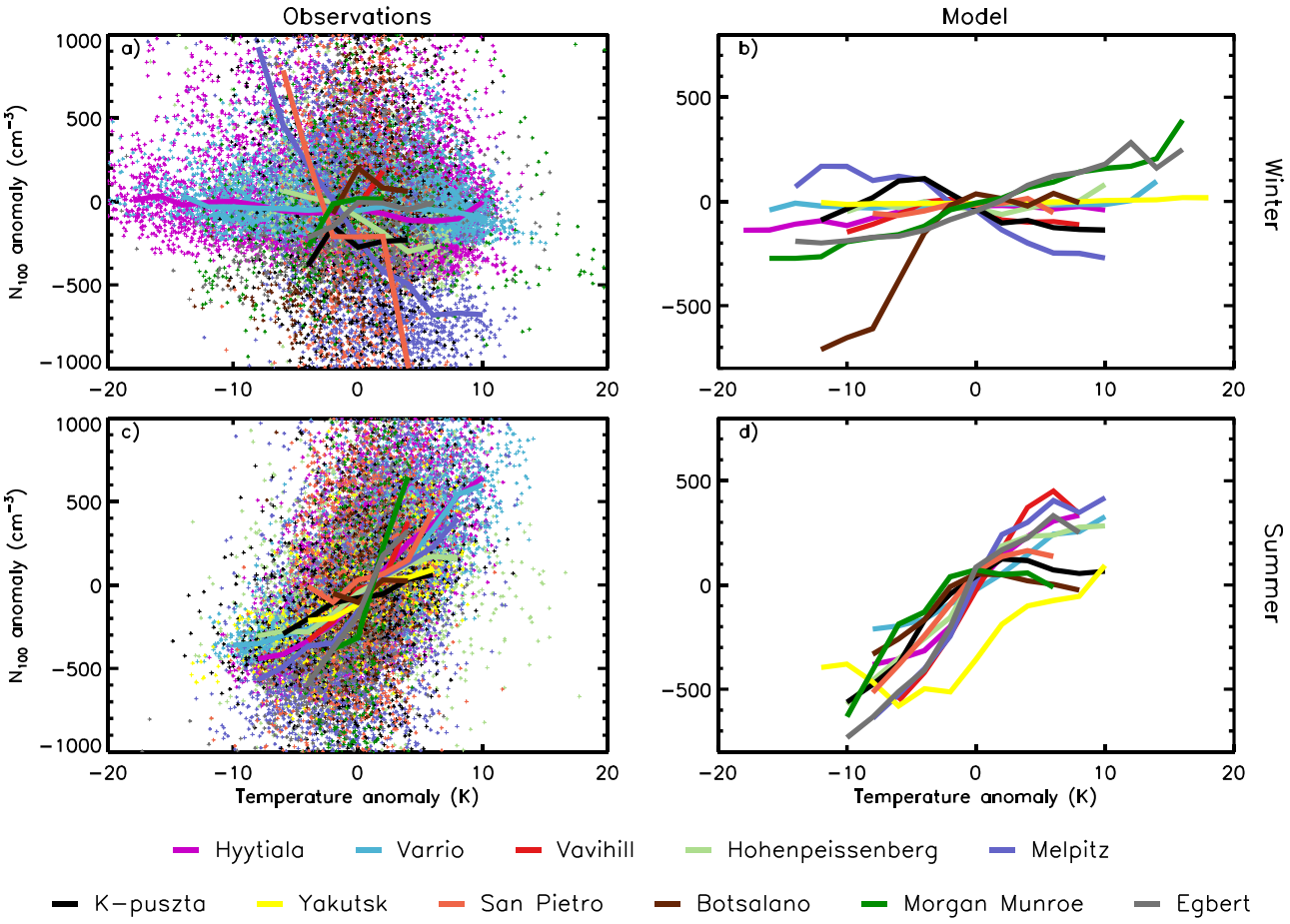
49 Dentener, F. *et al.* Emissions of primary aerosol and precursor gases in the years 2000 and 1750 prescribed data-sets for AeroCom. *Atmos. Chem. Phys.* **6**, 4321-4344, doi:10.5194/acp-6-4321-2006 (2006).

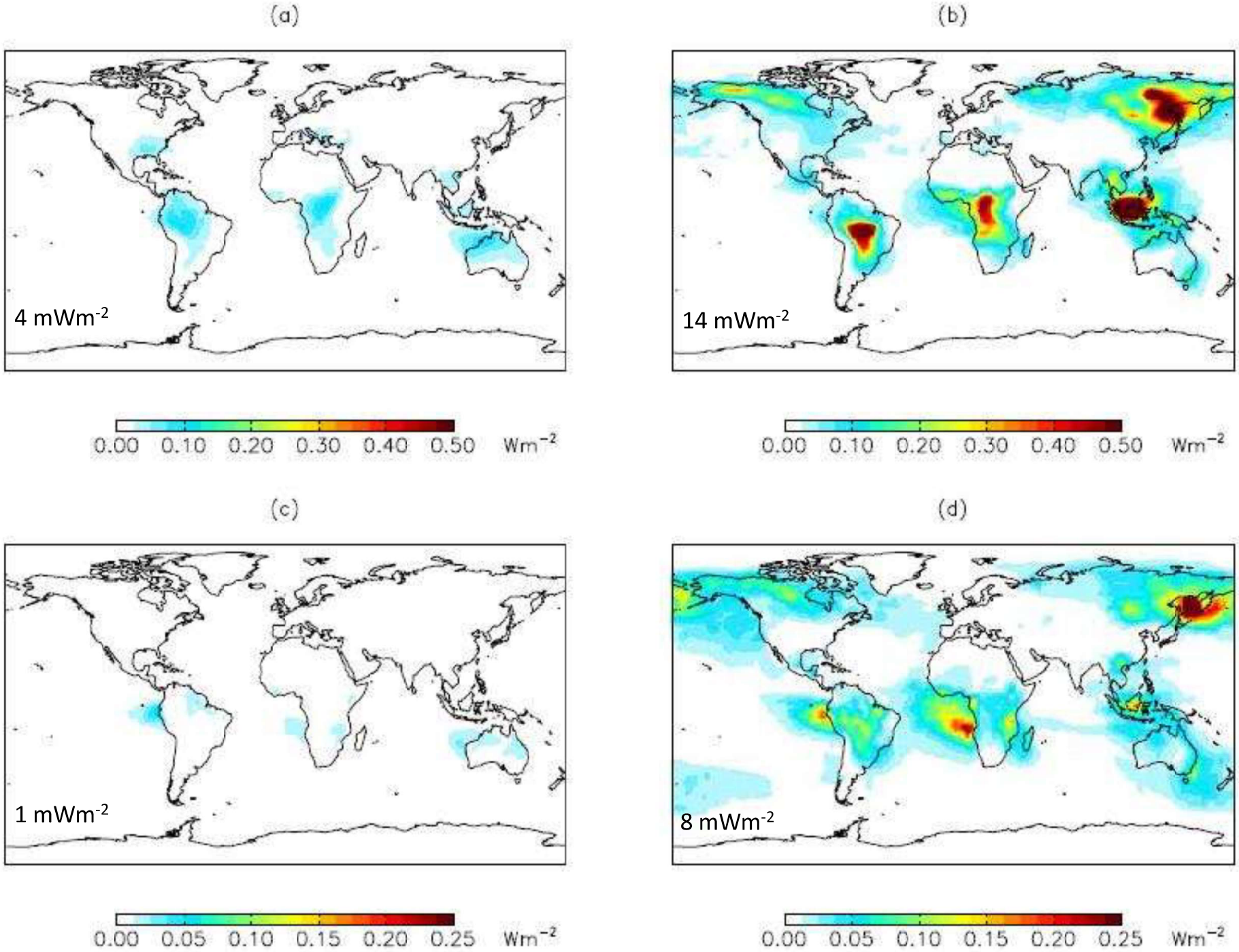
50 Mann, G. W. *et al.* Intercomparison of modal and sectional aerosol microphysics representations within the same 3-D global chemical transport model. *Atmos. Chem. Phys.* **12**, 4449-4476, doi:10.5194/acp-12-4449-2012 (2012).

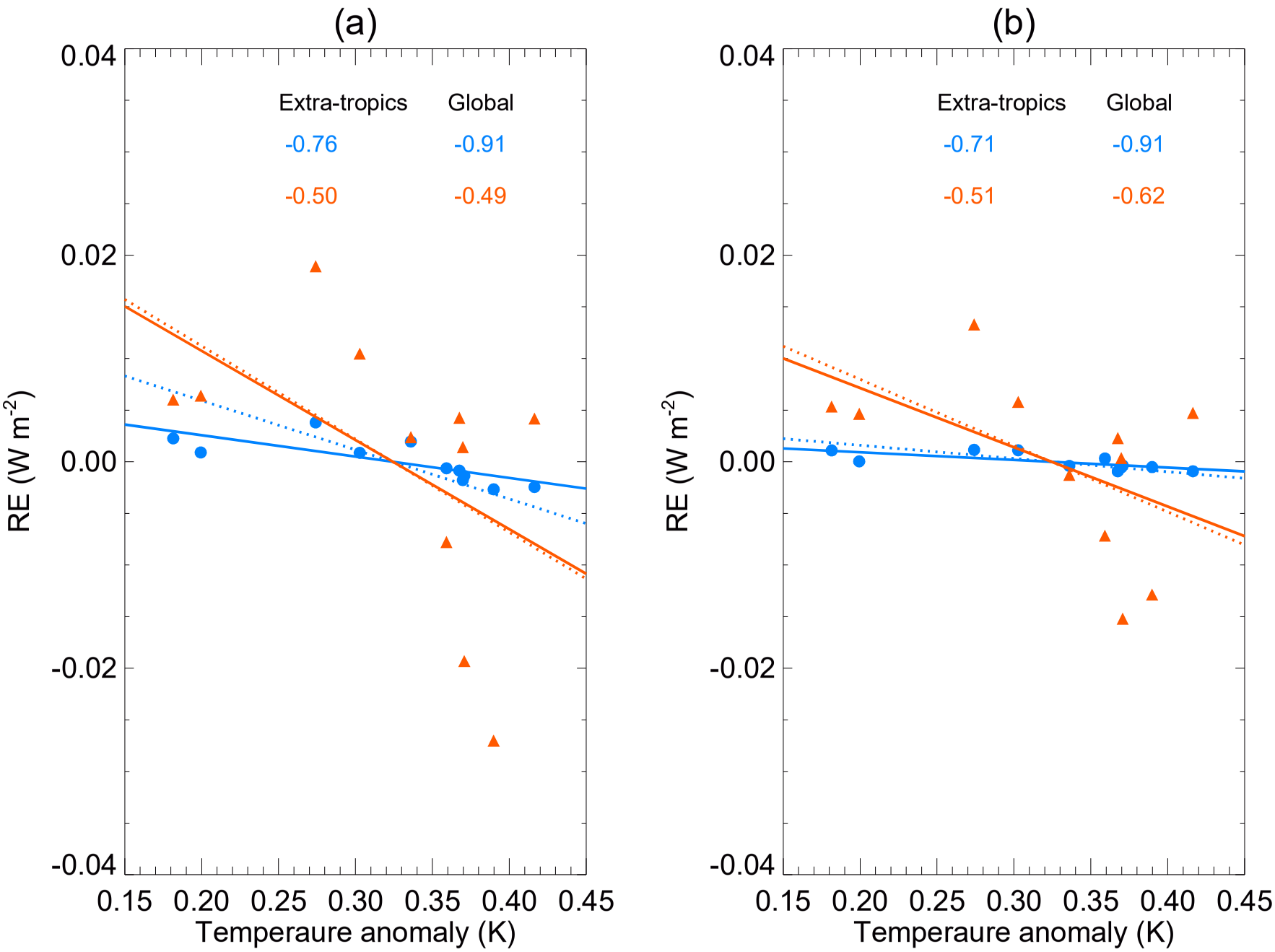
51 Metzger, A. *et al.* Evidence for the role of organics in aerosol particle formation under atmospheric conditions. *Proceedings of the National Academy of Sciences of the United States of America* **107**, 6646-6651, doi:10.1073/pnas.0911330107 (2010).

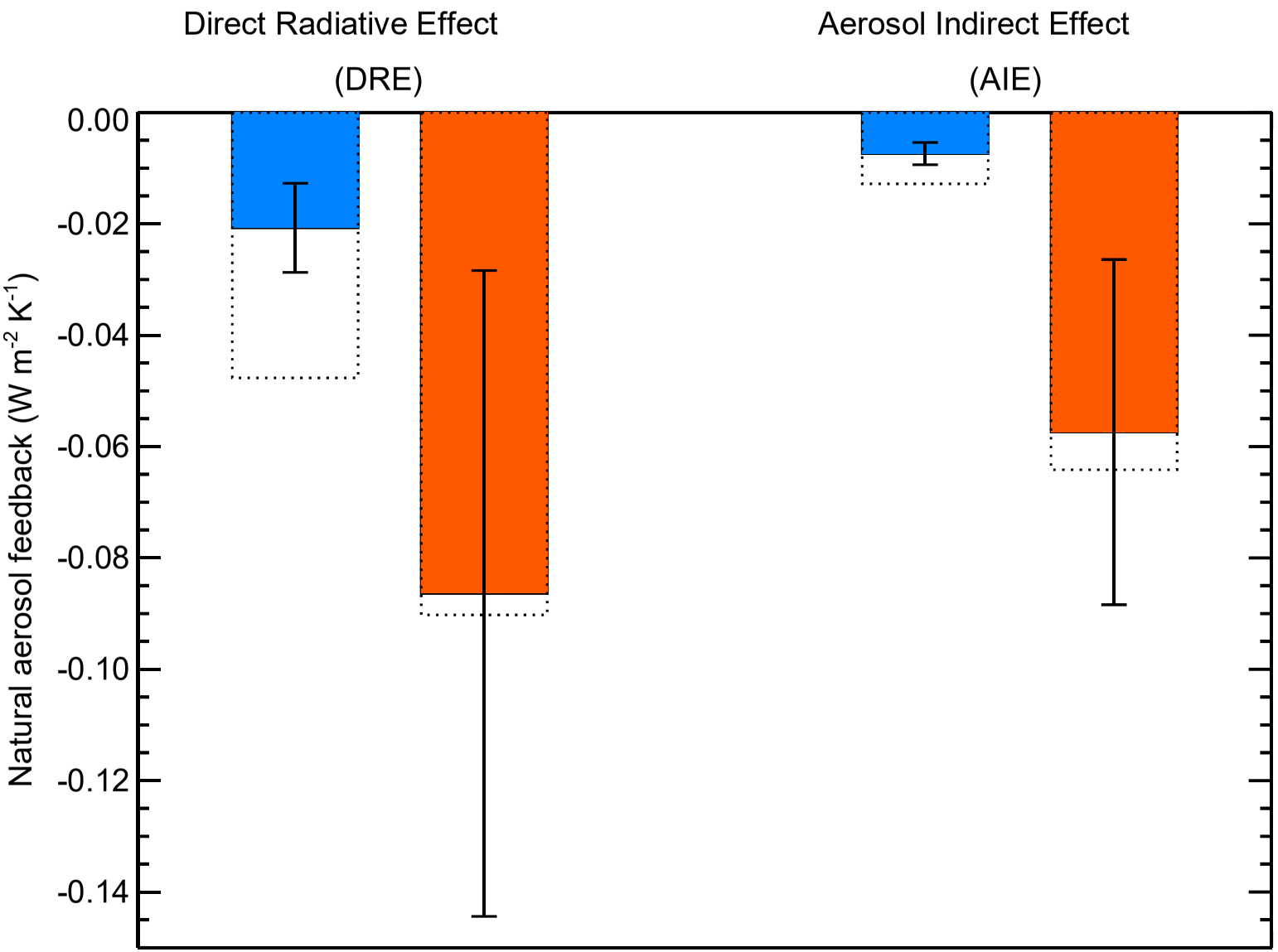
52 Edwards, J. M. & Slingo, A. Studies with a flexible new radiation code .1. Choosing a configuration for a large-scale model. *Q. J. R. Meteorol. Soc.* **122**, 689-719, doi:10.1002/qj.49712253107 (1996).

53 Smith, T. M., Reynolds, R. W., Peterson, T. C. & Lawrimore, J. Improvements to NOAA's Historical Merged Land–Ocean Surface Temperature Analysis (1880–2006). *Journal of Climate* **21**, 2283-2296, doi:10.1175/2007jcli2100.1 (2008).


Observations
Model
a)
b)
c)
d)
Winter
Summer
N_{100} anomaly (cm^{-3})
Temperature anomaly (K)
1000
500
0
−500
−1000
−20
−10
0
10
20
Hyytiala
Varrio
Vavihill
Hohenpeissenberg
Melpitz
K−puszta
Yakutsk
San Pietro
Botsalano
Morgan Munroe
Egbert


(a)
4 mWm-2
0.00 0.10 0.20 0.30 0.40 0.50 Wm-2
(b)
14 mWm-2
0.00 0.10 0.20 0.30 0.40 0.50 Wm-2
(c)
1 mWm-2
0.00 0.05 0.10 0.15 0.20 0.25 Wm-2
(d)
8 mWm-2
0.00 0.05 0.10 0.15 0.20 0.25 Wm-2


(a)
(b)
Extra-tropics
Global
-0.76
-0.91
-0.50
-0.49
-0.71
-0.91
-0.51
-0.62
RE (W m-2)
Temperaure anomaly (K)
0.04
0.02
0.00
-0.02
-0.04
0.15
0.20
0.25
0.30
0.35
0.40
0.45


Direct Radiative Effect
(DRE)
Aerosol Indirect Effect
(AIE)
0.00
-0.02
-0.04
-0.06
-0.08
-0.10
-0.12
-0.14
Natural aerosol feedback (W m-2 K-1)